X-ray emission in collisions of highly charged I, Pr, Ho, and Bi ions with a W surface

H. Watanabe,[1,2,*] J. Sun,[1] M. Tona,[1,2] N. Nakamura,[1] M. Sakurai,[3] C. Yamada,[1] N. Yoshiyasu,[1] and S. Ohtani[1,2]
[1]*Institute for Laser Science and Department of Applied Physics and Chemistry, University of Electro-Communications, Chofu, Tokyo 182-8585, Japan*
[2]*CREST, Japan Science and Technology Agency, Chofu, Tokyo 182-8585, Japan*
[3]*Department of Physics, Kobe University, Kobe, Hyogo, 657-8501, Japan*
(Received 19 April 2007; published 1 June 2007)

X-ray emission yields, which are defined as the total number of emitted x-ray photons per incident ion, and dissipated fractions of potential energies through x-ray emission have been measured for slow highly charged ions of I, Pr, Ho, and Bi colliding with a W surface. A larger amount of potential energy was consumed for the x-ray emission with increasing the atomic number and the charge state. The present measurements show that x-ray emission is one of the main decay channels of hollow atoms produced in collisions of very highly charged ions of heavy elements.

DOI: 10.1103/PhysRevA.75.062901 PACS number(s): 34.50.Dy, 32.30.Rj, 79.20.Rf

I. INTRODUCTION

The potential energy of a highly charged ion, which is the sum of the potential energies of all the electrons removed to make the ion, reaches several hundreds of keV for very highly charged ions of heavy elements. When the ion collides with a surface this energy is released instantaneously in a small area, which gives remarkable effects on the surface to cause a structural change of the surface [1–3]. In recent years, the studies of surface modification and nanostructure formation using these phenomena have been an active area of research [4]. There arises a question of how much of the potential energy is used for such surface modification.

The fractions of the potential energies deposited into a solid have been studied by Schenkel *et al.* [5]. Ne-like Au and He-like Xe were irradiated onto an ion implanted and passivated silicon detector, which has a 50 nm inactive contact layer in front of an active depletion region. Electron-hole pairs produced beyond this 50 nm inactive layer were measured. It was found that 35% and 40% of the potential energies of Ne-like Au and He-like Xe, respectively, were deposited in the depletion region of the detector. Kentsch *et al.* [6] has also measured the energy deposition of highly charged Ar^{q+} $(q=1-9)$ ions into a Cu target. They used a calorimetric method and measured the increase of temperature by deposition of the potential energy. They found that an average fraction of 30% to 40% of the potential energy was deposited in the solid with little dependence on the charge state. More recently with the same calorimetric method, the energy deposition of highly charged Ar ions into Cu and Si targets was measured and it was found that 80% of the potential energy was deposited into the solids [7]. From these results, it seems that for lower charge state ions the fraction of the potential energy deposited into a solid is large and with the increase of a charge state it becomes smaller.

When a highly charged ion approaches a surface, it captures electrons from the surface into its high Rydberg states and forms a highly excited atom with inner shell vacancies, which is called a hollow atom [8]. X rays from hollow atoms have been measured to study production and decay mechanisms of hollow atoms. In the early studies of x-ray emission from hollow atoms, significant efforts have been devoted to measure x-ray transition energies with a crystal spectrometer and a Si(Li) detector [9–12]. Due to the clock property of hollow atoms, the shape of the x-ray spectrum changes depending on the spatial position where formation and decay of the hollow atoms take place. These studies have made the understanding of the production and decay mechanisms of hollow atoms much deeper. On the other hand, only a few measurements have been reported about x-ray intensity [13–16], or x-ray emission yield of hollow atoms, which is defined as the total number of emitted x-ray photons per incident ion. Ninomiya *et al.* [13,14] reported *L* x-ray emission yields for highly charged Ar ions with *L*-shell vacancies impinged on several kinds of targets. The observed x-ray intensity was less than 0.002 counts per incident ion. They showed that only a small amount of x rays was emitted from the hollow atoms of Ar ions. This fact does not contradict the results of the recent calorimetric observations that 80% of the potential energy was deposited into the solid [7]. Thus in the case of the highly charged Ar-surface collisions a large portion of the potential energy was deposited into the solid and a much smaller portion was dissipated through x-ray emission.

In a previous paper we reported x-ray emission yields and dissipated fractions of the potential energies through x-ray emission for the collision between highly charged I ions and a hydrogen terminated silicon (111) surface [16]. It was found that almost 100% of the *K*-shell and about 20% of the *L*-shell were filled through x-ray emission nearly irrespective of the number of vacancies, while the *M*-shell was filled almost nonradiatively. As a result, a clear shell structure was observed in the dissipated fractions of the potential energies through x-ray emission. For the ions with only *M*-shell vacancies, the dissipated fractions of the potential energies through x-ray emission are approximately zero. With increasing *L*-shell vacancies, they increase gradually and reach 10% for He-like ions. Once the *K*-shell has a vacancy, 30%–40% of the potential energy dissipates through x-ray emission.

In this paper, we report *L* and *M* x-ray emission yields and dissipated fractions of the potential energies through x-ray emission not only for I, but also for much heavier

*Electronic address: h_watana@ils.uec.ac.jp

elements than I which was used in the previous study. Highly charged ions up to He-like ions of I (Z=53), Pr (Z=59), Ho (Z=67), and Bi (Z=83) were used as projectiles and a W surface as a target. Because K x-ray emission yields are almost 100% even for I at Z=53, which is much lighter than Pr, Ho, and Bi, observations were limited up to He-like ions of these elements which do not have K-shell vacancies [16]. We show the significance of L and M x-ray emission as a decay channel of hollow atoms of very high Z elements.

II. EXPERIMENT

The experimental setup was almost the same as the previous study [16]. An electron beam ion trap (EBIT) at the University of Electro-Communications, the Tokyo-EBIT [17], was used to produce highly charged ions of I, Pr, Ho, and Bi. The source atoms of Pr, Ho, and Bi were introduced into the trap as metal vapors with an effusion cell [18] and that of I was introduced as CH_3I. These atoms were ionized by successive electron impacts of the electron beam of the EBIT with the energy of 63 keV and the current of 125 mA. The produced ions were extracted with 3 kV electrostatic potential from the trap, mass-analyzed with a sector magnet, and then introduced into a target chamber. The target was a W surface, which was biased by −500 V electrostatic potential to the ground potential. Therefore the energy of the ions colliding with the target was $3.5\times q$ keV. Before measurements, the W surface was cleaned by irradiating an Ar^+ beam of about 0.8 μA for several minutes.

X rays emitted from the hollow atoms produced by the ion-surface collisions were detected with a Si(Li) detector at 60° from the ion beam axis. The detected x-ray signal was accumulated with a multichannel analyzer (MCA).

More than 100 secondary electrons are emitted by a single highly charged ion impact on a surface [19]. These electrons accelerated by the −500 V bias voltage were detected with an annular-type microchannel plate (MCP), which faced the target. This signal was used to count the number of incident ions without miscounts [20] and also used as a gate signal for the MCA not to accumulate noise signals in the obtained spectra.

III. RESULTS AND DISCUSSION

Spectra of He-like to Ne-like Bi are shown in Fig. 1. The energy scale of the spectra was calibrated with x rays from the radioisotopes of ^{241}Am and ^{55}Fe. The solid angle subtended by the detector was 8.9 msr. The detection efficiency of the detector was known in the energy range between 1 and 25 keV [16]. The spectra were corrected by the solid angle and the detection efficiency, and then normalized by the number of incident ions and the x-ray energy width corresponding to one channel of the MCA. Therefore in Fig. 1 the area enclosed by the spectral curve and the horizontal axis is the total number of emitted x rays per incident ion. It should be noted that x-ray intensity in the range below 1 keV was weak due to strong attenuation by the Be window of the detector. The x rays in this range were truncated because correction by the transmission of a Be window causes a large error in the x-ray emission yields.

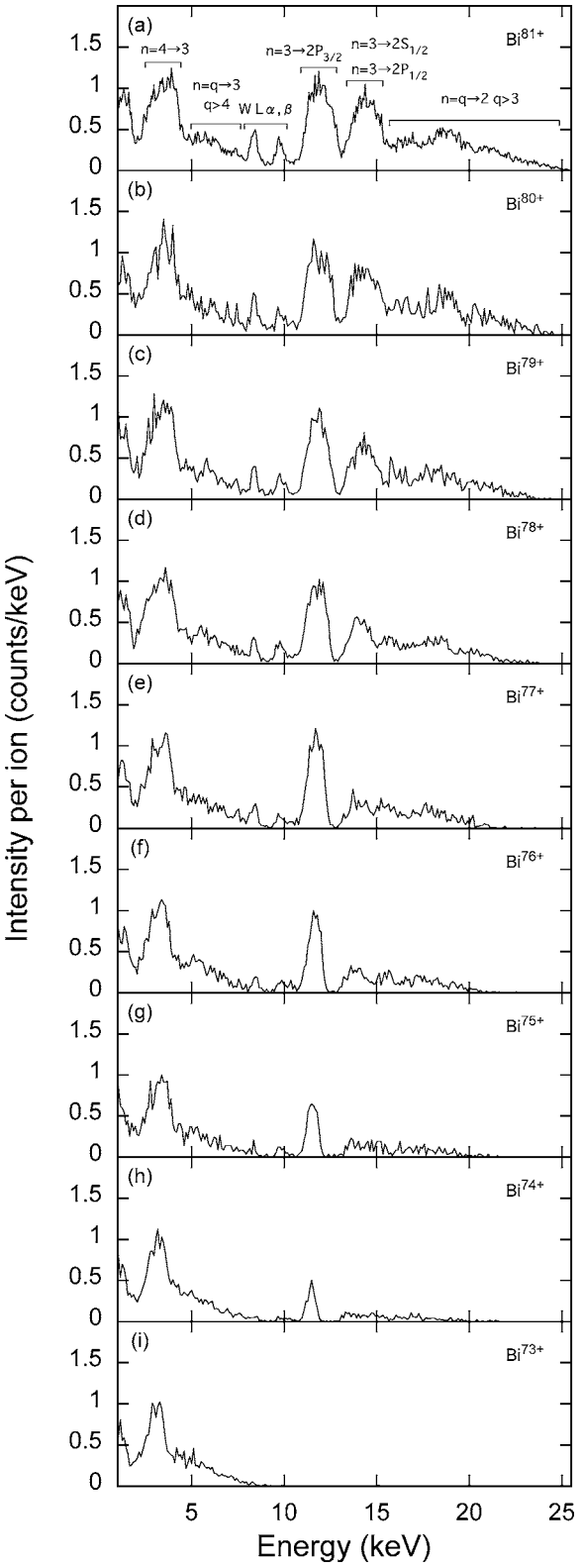

FIG. 1. (a)–(i) X-ray spectra of Bi following $3.5\times q$ keV Bi^{q+} (q=73−81) ion impact on a W surface.

As can be seen, the Bi^{81+} spectrum consists of M x-ray peaks between 2 and 8 keV and L x-ray peaks above 10 keV.

Between these regions two peaks were observed at 8.4 and 9.7 keV, which were identified as $L\alpha$ and $L\beta$ x rays of W. Since the energy of L x rays of Bi is just above the L-edge of W, L x rays are absorbed efficiently by W. The absorbed x rays were reemitted from the W target as fluorescence.

In the region of L x rays, two prominent peaks were observed at 12 and 14.5 keV. With increasing the charge state, the structure of the spectra changes. The peak at 12 keV appears from Bi^{74+} together with a small and wide "bump" beyond 13 keV, while the peak at 14.5 keV seems to appear from Bi^{78+} on the bump. Because the level $2p_{3/2}$ is the highest in $n=2$, the vacancies in $2p_{3/2}$ open from Bi^{74+}. The peak at 12 keV is assigned to be the transitions from $n=3$ to $2p_{3/2}$ and the bump on the high energy side corresponds to the transitions from states higher than $n=3$ to $2p_{3/2}$. As the increase of the charge state, vacancies in $2p_{1/2}$ open from Bi^{78+} and those in $2s_{1/2}$ from Bi^{80+}, transitions to which from $n=3$ make the peak at 14.5 keV superimposed on the bump. The separation between these two peaks corresponds to the energy difference between $2p_{3/2}$ and $2p_{1/2}$ (fine structure) [21]. The energy difference between $2p_{1/2}$ and $2s_{1/2}$ (Lamb shift) is too small for the detector resolution, so the transitions from $n=3$ to these states could not be resolved.

In contrast to L x rays, the structure of M x rays in these spectra seems rather simple due to the detector resolution. However, with increasing the charge state, the higher energy side of the peak structure becomes broader and complex, which is a contribution from the hollow atoms with more M-shell vacancies. It is noticed that each spectrum looks like a subset of the spectrum of higher charge state ions. This might be because the outer electron configuration for each step of the transitions reaches equilibrium at the time of x-ray emissions. This feature was also observed in the spectra of the other projectiles.

The spectra of He-like I, Pr, and Ho are shown in Figs. 2(a)–2(c). Because the separations of energy levels are small, transitions to different fine structure levels could not be resolved. Accordingly, the structure of the spectra becomes rather simple and similar to each other even for the different elements. The highest peak corresponds to $L\alpha$ x rays ($n=3\rightarrow 2$), which has a subcomponent on the high-energy side corresponding to L x rays from higher states than $n=3$. The second highest peak is $M\alpha$ x rays, which also has a tail of x rays from higher states.

We have obtained L and M x-ray emission yields for each element by numerically integrating the areas below the spectral features from 2.2 to 7.9 keV and from 11.7 to 26.7 keV for Bi, from 1.0 to 6.5 keV and from 6.5 to 16.1 keV for Ho, from 1 to 4.6 keV and from 4.7 to 12.7 keV for Pr, and from 1.0 to 3.7 keV and from 3.7 to 9.6 keV for I for M and L x rays, respectively. The uncertainties due to the counting statistics, the detection efficiency, and the observation solid angle were taken into account in estimating the error bars. It should be noted that the M x-ray emission yields might have additional uncertainties due to the truncation of the x rays below 1 keV.

X-ray emission yields for I, Ho, and Bi are shown in Figs. 3(a)–3(c). Common features of change of the x-ray emission yields with the charge state q are as follows; L x rays appear from F-like ions with one L-shell vacancy and increases steeply with q, while M x rays increase gradually. This increase is almost linear with q for L x rays, which means that the emission yields of L x rays increase linearly with the number of vacancies in the lower shell of the transitions. In the case of M x rays, the rate of the increase changes at F-like ions. The maximum number of M-shell vacancies is eight at Ne-like ions. However, once an L-shell vacancy opens, M-shell population would be transferred at a certain rate to the L-shell, which, in effect, opens additional vacancies in the M-shell and, thus, more than eight M transitions could take place. By an LMM Auger transition two additional vacancies are produced, while by an $L\alpha$ transition and an LMx ($x=N,O,\ldots$), Auger transition one additional vacancy. As seen in the figures, L x-ray emission yields of Bi are much larger than those of I, reflecting the fact that the fluorescence yields increase with Z. This means, inversely, that the filling probability of the L-shell by Auger transitions in Bi is smaller than that in I. Therefore the increase of M-shell vacancies in Bi due to the transitions to the L-shell is

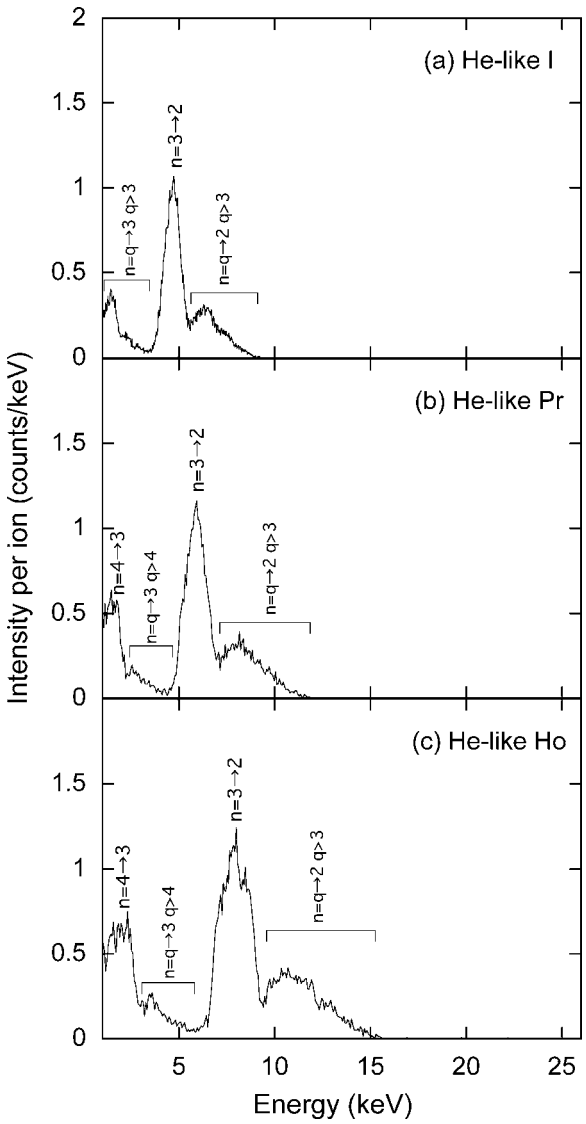

FIG. 2. X-ray spectra observed with (a) He-like I, (b) He-like Pr, and (c) He-like Ho.

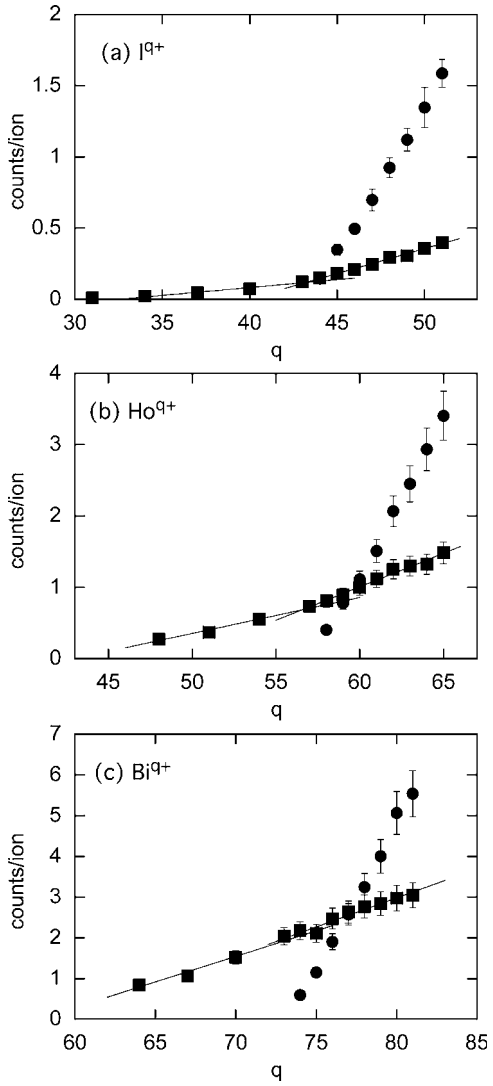

FIG. 3. X-ray emission yields as a function of the projectile charge q from (a) I, (b) Ho, and (c) Bi ions; circles: L x-ray emission yields and squares: M x-ray emission yields. The lines are shown to guide the eye.

smaller than that in I, which makes the change of slopes for Bi smaller than that for I.

As is seen from Figs. 3(a)–3(c), the x-ray emission yields becomes larger with the atomic number. For example, x-ray emission yield of He-like I is about 1.6, while that of He-like Bi is about 5.5. These values are summarized for He-like ions in Fig. 4. The left axis is the x-ray emission yield and the right axis is the fluorescence yield that is obtained by dividing the x-ray emission yield by the number of vacancies in the L-shell, that is, eight, which is a radiative filling probability of vacancies. In the case of I, only about 20% of the vacancies are filled by x-ray transitions, which means that about 80% are filled by nonradiative transitions. On the other hand, in the case of Bi, about 70% of the vacancies are filled by x-ray transitions and about 30% are by nonradiative transitions. These results indicate that radiative transitions play an important role in filling vacancies of very highly charged ions of heavy elements.

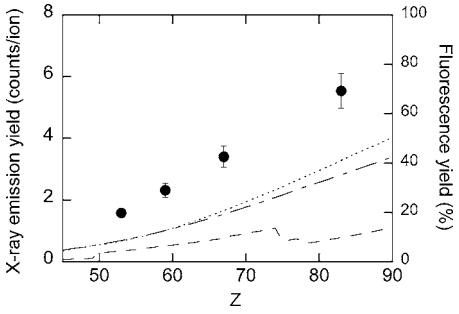

FIG. 4. X-ray emission yields and fluorescence yields of He-like I (Z=53), Pr (Z=59), Ho (Z=67), and Bi (Z=83). The lines are Dirac-Hartree-Slater predictions [22] of atomic L subshell fluorescence yields as a function of the projectile atomic number Z; dashed line: $L1$ subshell fluorescence yield; dotted line: $L2$ subshell fluorescence yield; and dot-dashed line: $L3$ subshell fluorescence yield.

In Fig. 4 atomic fluorescence yields for $L1$ ($2s_{1/2}$), $L2$ ($2p_{1/2}$), and $L3$ ($2p_{3/2}$) subshells are also shown, calculated by the Dirac-Hartree-Slater method [22]. The fluorescence yields of the present measurements are approximately twice as large as the atomic fluorescence yields for the $L2$ and $L3$ subshells. In the case of hollow atoms the effective nuclear charge which is seen by the electrons in upper states before transition is much larger than in the case of atoms. This makes the radiative transition rates larger, while the Auger rates do not strongly depend on the nuclear charge [23]. Therefore the fluorescence yields of hollow atoms become much larger than the atomic fluorescence yields. A similar increase was observed for the K-shell fluorescence yields [10,16,24]. It can be said that the increase of the fluorescence yields is one of the characteristics of hollow atoms.

Figure 5 shows the dissipated fractions of the potential energies through x-ray emission as a function of Z for selected isoelectronic sequences of projectile ions. These values were obtained by dividing the total emitted x-ray energy by the potential energy of ions [25]. He-like and C-like ions have L-shell vacancies, while Ne-like and Al-like ions do not but have M-shell vacancies. If Z is fixed, these fractions increase from Al-like to He-like ions, though the rate of increase becomes larger from Ne-like to He-like than those from Al-like to Ne-like. Clear shell dependence is seen,

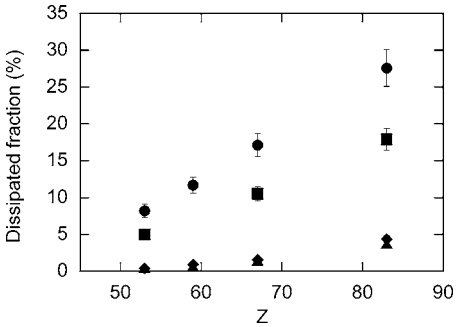

FIG. 5. The dissipated fractions of the potential energy through x-ray emission for different charge state ions of I (Z=53), Pr (Z=59), Ho (Z=67), and Bi (Z=83); circles: He-like; squares: C-like; diamonds: Ne-like; and triangles: Al-like.

which comes from the fact that ions with *L*-shell vacancies from F-like to He-like can emit *L* x rays with higher yields and energies as the charge state increases.

It has been recognized that for low *Z* and low *q* ions such as Ar^{q+}, a large fraction of the potential energy was retained into the target (80%) to be finally transferred into heat [7], while for higher *Z* and higher *q* ions such as He-like Xe and Ne-like Au the fractions of the potential energies retained into the targets became lower (40% and 35%) [5]. On the other hand, the dissipated fraction of the potential energy through x-ray emission becomes larger both with *Z* and *q*. In the case of He-like ions, about 28% of the potential energy dissipates through x-ray emission for Bi, while about 8% for I. This steep increase with *Z* shows the importance of x-ray emission in the decay channels of hollow atoms produced by the collisions of very highly charged ions of heavy elements with a surface.

IV. SUMMARY

We have measured x-ray emission yields and dissipated fractions of the potential energies through x-ray emission for slow highly charged ions of I, Pr, Ho, and Bi which collide with the W surface. The x-ray emission yields of *L* and *M* x rays increase with atomic number, for *L* x rays, from 1.6 counts per incident ion for He-like I to 5.5 for He-like Bi, and for *M* x rays from 0.41 to 3.0, respectively. For the heaviest element we have studied, i.e., for He-like Bi ($Z=83$), as much as 28% of the potential energy dissipated through x-ray emission. The present observation shows that x-ray emission becomes one of the main decay channels of hollow atoms produced in collisions of highly charged ions with high *Z* and *q*.

ACKNOWLEDGMENTS

This work was performed under the auspices of the CREST program, "Creation of Ultra-fast, Ultralow Power, Super-performance Nanodevices and Systems" of the Japan Science and Technology Agency. This work was a part of the 21st Century Center of Excellence Program, "Innovation in Coherent Optical Science" at the University of Electro-Communications, and the Reimei (Dawn) Research Promotion Project of Japan Atomic Energy Agency (JAEA).

[1] G. Borsoni, M. Gros-Jean, M. L. Korwin-Pawlowski, R. Laffitte, V. Le Roux, and L. Vallier, J. Vac. Sci. Technol. B **18**, 3535 (2000).
[2] Y. Baba, K. Nagata, S. Takahashi, N. Nakamura, N. Yoshiyasu, M. Sakurai, C. Yamada, S. Ohtani, and M. Tona, Surf. Sci. **599**, 248 (2005).
[3] M. Tona, H. Watanabe, S. Takahashi, N. Nakamura, N. Yoshiyasu, M. Sakurai, T. Terui, S. Mashiko, C. Yamada, and S. Ohtani, Surf. Sci. **601**, 723 (2007).
[4] J. D. Gillaspy, J. Phys. B **34**, R93 (2001).
[5] T. Schenkel, A. V. Barnes, T. R. Niedermayr, M. Hattass, M. W. Newman, G. A. Machicoane, J. W. McDonald, A. V. Hamza, and D. H. Schneider, Phys. Rev. Lett. **83**, 4273 (1999).
[6] U. Kentsch, H. Tyrroff, G. Zschornack, and W. Möller, Phys. Rev. Lett. **87**, 105504 (2001).
[7] D. Kost, S. Facsko, and R. Hellhammer, in book of abstracts of the *Thirteenth International Conference on the Physics of Highly Charged Ions, 2006*, edited by J. T. Costello, G. F. Gribakin, M. P. Scott, and E. Sokell (Queen's University, Belfast, 2006), p. 3–14.
[8] HP. Winter and F. Aumayr, J. Phys. B **32**, R39 (1999).
[9] J. P. Briand, L. de Billy, P. Charles, S. Essabaa, P. Briand, R. Geller, J. P. Desclaux, S. Bliman, and C. Ristori, Phys. Rev. Lett. **65**, 159 (1990).
[10] J. P. Briand, B. d'Etat-Ban, D. Schneider, M. A. Briere, V. Decaux, J. W. McDonald, and S. Bardin, Phys. Rev. A **53**, 2194 (1996).
[11] J. P. Briand, S. Thuriez, G. Giardino, G. Borsoni, M. Froment, M. Eddrief, and C. Sébenne, Phys. Rev. Lett. **77**, 1452 (1996).
[12] J. P. Briand, G. Giardino, G. Borsoni, M. Froment, M. Eddrief, C. Sébenne, S. Bardin, D. Schneider, J. Jin, H. Khemliche, Z. Xie, and M. Prior, Phys. Rev. A **54**, 4136 (1996).
[13] S. Ninomiya, Y. Yamazaki, K. Sawatrai, M. Irako, K. Komaki, T. Azuma, K. Kuroki, and M. Sekiguchi, Nucl. Instrum. Methods Phys. Res. B **115**, 177 (1996).
[14] S. Ninomiya, Y. Yamazaki, T. Azuma, K. Komaki, K. Kuroki, and M. Sekiguchi, Nucl. Instrum. Methods Phys. Res. B **135**, 82 (1998).
[15] G. A. Machicoane, T. Schenkel, T. R. Niedermayr, M. W. Newmann, A. V. Hamza, A. V. Barnes, J. W. McDonald, J. A. Tanis, and D. H. Schneider, Phys. Rev. A **65**, 042903 (2002).
[16] H. Watanabe, S. Takahashi, M. Tona, N. Yoshiyasu, N. Nakamura, M. Sakurai, C. Yamada, and S. Ohtani, Phys. Rev. A **74**, 042901 (2006).
[17] H. Watanabe, J. Asada, F. J. Currell, T. Fukami, T. Hirayama, K. Motohashi, N. Nakamura, E. Nojikawa, S. Ohtani, K. Okazaki, M. Sakurai, H. Shimizu, N. Tada, and S. Tsurubuchi, J. Phys. Soc. Jpn. **66**, 3795 (1997).
[18] C. Yamada, K. Nagata, N. Nakamura, S. Ohtani, S. Takahashi, T. Tobiyama, M. Tona, H. Watanabe, N. Yoshiyasu, M. Sakurai, A. P. Kavanagh, and F. J. Currell, Rev. Sci. Instrum. **77**, 066110 (2006).
[19] F. Aumayr, H. Kurz, D. Schneider, M. A. Briere, J. W. McDonald, C. E. Cunningham, and HP. Winter, Phys. Rev. Lett. **71**, 1943 (1993).
[20] N. Yoshiyasu, S. Takahashi, M. Shibata, H. Shimizu, K. Nagata, N. Nakamura, M. Tona, M. Sakurai, C. Yamada, and S. Ohtani, Jpn. J. Appl. Phys., Part 1 **45**, 995 (2006).
[21] M. H. Chen, K. T. Cheng, W. R. Johnson, and J. Sapirstein, Phys. Rev. A **52**, 266 (1995).
[22] J. L. Campbell, At. Data Nucl. Data Tables **85**, 291 (2003).
[23] H. F. Beyer and V. P. Shevelko, *Introduction to the Physics of Highly Charged Ions* (Institute of Physics Publishing, Bristol, 2003), pp. 186–201.
[24] T. Schenkel, A. V. Hamza, A. V. Barnes, and D. H. Schneider, Prog. Surf. Sci. **61**, 23 (1999).
[25] T. A. Carlson, C. W. Nestor, Jr., N. Wasserman, and J. D. McDowell, At. Data **2**, 63 (1970).